AIP | The Journal of Chemical Physics

Operational electrochemical stability of thiophene-thiazole copolymers probed by resonant Raman spectroscopy

Jessica Wade, Sebastian Wood, Daniel Beatrup, Michael Hurhangee, Hugo Bronstein, Iain McCulloch, James R. Durrant, and Ji-Seon Kim

Citation: The Journal of Chemical Physics **142**, 244904 (2015); doi: 10.1063/1.4923197
View online: http://dx.doi.org/10.1063/1.4923197
View Table of Contents: http://scitation.aip.org/content/aip/journal/jcp/142/24?ver=pdfcov
Published by the AIP Publishing

Operational electrochemical stability of thiophene-thiazole copolymers probed by resonant Raman spectroscopy

Jessica Wade,[1] Sebastian Wood,[1] Daniel Beatrup,[2] Michael Hurhangee,[2] Hugo Bronstein,[2,3] Iain McCulloch,[2] James R. Durrant,[2] and Ji-Seon Kim[1,a)]
[1]*Department of Physics and Centre for Plastic Electronics, Imperial College London, London SW7 2AZ, United Kingdom*
[2]*Department of Chemistry and Centre for Plastic Electronics, Imperial College London, London SW7 2AY, United Kingdom*
[3]*Department of Chemistry, University College London, London WC1H 0AJ, United Kingdom*

(Received 31 March 2015; accepted 17 June 2015; published online 30 June 2015)

We report on the electrochemical stability of hole polarons in three conjugated polymers probed by resonant Raman spectroscopy. The materials considered are all isostructural to poly(3-hexyl)thiophene, where thiazole units have been included to systematically deepen the energy level of the highest occupied molecular orbital (HOMO). We demonstrate that increasing the thiazole content planarizes the main conjugated backbone of the polymer and improves the electrochemical stability in the ground state. However, these more planar thiazole containing polymers are increasingly susceptible to electrochemical degradation in the polaronic excited state. We identify the degradation mechanism, which targets the C=N bond in the thiazole units and results in disruption of the main polymer backbone conjugation. The introduction of thiazole units to deepen the HOMO energy level and increase the conjugated backbone planarity can be beneficial for the performance of certain optoelectronic devices, but the reduced electrochemical stability of the hole polaron may compromise their operational stability. © *2015 AIP Publishing LLC.* [http://dx.doi.org/10.1063/1.4923197]

I. INTRODUCTION

To fully realise the commercialisation of organic electronics, there is an urgent need to address the issue of stability and lifetime. Degradation studies of polymer electronic devices are increasingly reported in the literature, where various types of stability have been considered, including chemical and morphological degradation of active layer under various conditions.[1,2] However, there has been very little study on the operational stability of the charge carriers injected into the active material of polymer devices. The energy level of the highest occupied molecular orbital (HOMO) represents the energy required to remove an electron from a neutral molecule, so at this potential, charge (hole) is injected into the polymer forming a hole polaron, and the polymer is reversibly oxidised. When used as an electron donor, polymers with a similar lowest unoccupied molecular orbital (LUMO) energy level but a deeper HOMO level are reported to improve organic photovoltaic performance due to their increased energy level offsets with fullerene LUMO, and improve their stability to electrochemical reactions in air.[3–5]

Poly(3-hexyl)thiophene (P3HT) is one of the most widely studied polymer materials, and remains important for fundamental studies in the field of organic photovoltaics and in tandem solar cells.[6–9] Stability/degradation of P3HT has been investigated extensively and its consequences are well-documented, yet the mechanism is still under debate.[10–13] In general, exposure to light, heat, or oxygen can destroy the π-conjugation of P3HT and reduce light absorption.[11,12,14] Singlet oxygen is understood to degrade polymer solutions, whilst in the solid-state it is proposed that the alkyl side chains are attacked leading to a reactive peroxide species which oxidises the sulphur and breaks apart the thiophene ring.[10,14–16] Madsen *et al.* compared the stability of regioregular (RR) and regiorandom (RRa) P3HT under simulated sunlight and found that photo-degrading radicals attack the polymer at points in the chain where conformational conjugation is broken.[17]

II. MATERIALS AND METHODS

A. Materials

In our previous work, we compared the electrochemical stability to oxidative stress of three polymers with different HOMO energy levels.[18,19] We reported that incorporation of thiazole into a thiophene chain systematically deepens the HOMO level, and that these materials were less chemically stable in the polaronic state. The three polymers considered here are copolymers of thiophene and thiazole with different proportions: P3HT is all thiophene units, poly(2-(3',4-dihexyl-[2,2'-bithiophen]-5-yl)-4-hexylthiazole (PTTTz) has every third unit substituted with thiazole, and poly(4-hexyl-2-(3-hexylthiophen-2-yl)thiazole) (PTTz) has alternate units substituted with thiazole (Figure 1). Here, we aim to experimentally probe the mechanism behind this observation.

Thiazole is a commonly used electron-accepting heterocyclic compound due to electron-withdrawing nitrogen in the C=N bond.[4,20,21] The systematic introduction of thiazole

a)Author to whom correspondence should be addressed. Electronic mail: ji-seon.kim@imperial.ac.uk

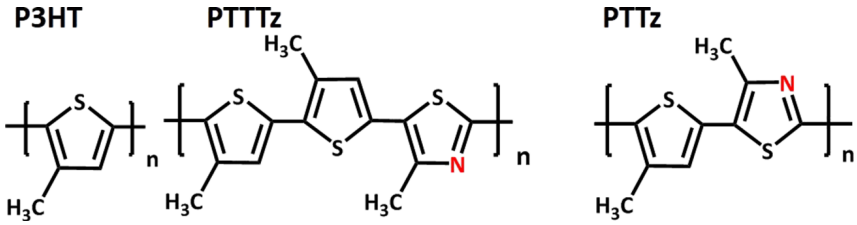

FIG. 1. Chemical structures of the three polymers (P3HT, PTTTz, and PTTz) studied in this work.

units into the thiophene chain deepens the HOMO level and reduces steric interactions between the adjacent heterocycles (removes C—H···C—H interactions) leading to a more planar conjugated backbone structure.[4] The anti-bonding (π*) orbital energy levels of the electron-withdrawing thiazole units are similar to those of other π-conjugated materials, resulting in efficient mixing of orbitals and a deeper LUMO level.[4,21] Bronstein *et al.* proposed an interaction between the nitrogen lone pair and adjacent C—S anti-bonding orbitals in neighbouring backbone units leading to a stable planar configuration in polymers containing thiazole units, which reduces the width of the density of conformational states.[18] However, their study is limited to theoretical analysis of molecular conformations using density functional theory (DFT). Yamamoto *et al.* use XRD to measure changes in π-stacking when alkylated thiazole is introduced into a chain of thiophene units.[20] They reveal a reduction in π-stacking distance from 4.2 Å in PTh(R)Th to 3.65 Å in PTz(R)Th, which is consistent with an increase in molecular planarity, though an indirect measure.[20] Here, we provide a more direct experimental analysis using Raman spectroscopy to confirm these other studies.

B. Methods

The three polymers have different HOMO energy levels (P3HT, −4.8 eV; PTTTz, −5.1 eV; and PTTz, −5.2 eV from CV) and so require different potentials to inject holes.[19] We control the degree of polymer electrochemical oxidation using chronoamperometry at different potentials in order to apply the same polaron density (10^{20} cm^{-3}) to each sample, thus to ensure the different polymers are subjected to the same extent of oxidative stress (see below for details).[19] We have reported on the use of this method elsewhere, where *in situ* absorption spectra were used to monitor the extent of electrochemical degradation.[19] Whilst UV-visible absorption measurements can provide some evidence for morphological differences and optical property changes in the polymer thin film due to the degradation effect, it provides limited information about the chemical and conformational changes at a molecular level. To investigate this further, we have employed resonant Raman spectroscopy, which is sensitive to molecular structure and conformation.[22–31] We have previously demonstrated the use of resonant Raman spectroscopy to quantify the degree of molecular order in P3HT induced by thermally annealing P3HT: fullerene blend films.[25]

1. Film preparation

Films were spin-coated from solutions of polymer dissolved in chlorinated solvent (chloroform for P3HT, chlorobenzene for PTTTz, *ortho*-dichlorobenzene for PTTz). fluorine-doped tin oxide (FTO)/glass substrates were covered with polymer solution, before being spun at 2000 rpm, for 1 min, under a nitrogen atmosphere. Films were then dried under vacuum overnight.

2. Chronoamperometry

Measurements were carried out in a 3-electrode spectroelectrochemical cell, consisting of a platinum gauze counter electrode, Ag/AgCl reference electrode, with the polymer film/FTO/glass substrate forming the working electrode, as well as two quartz windows suitable for absorption spectroscopy measurements. The working electrode was held in a neutral state by applying a starting potential (V_0) of 0.00 V. This was followed by applying an oxidising potential (V_{probe}) of +0.65 V, +0.80 V, and +1.05 V to the working electrode, for P3HT, PTTTz, and PTTz, respectively (all potentials quoted with respect to Ag/AgCl reference electrode), for 10 000 s (just under 3 h). This oxidising potential was used to electrochemically degrade the polymer film, after which the film was returned to its neutral state, by reducing the applied potential to 0.00 V. Subsequently, absorption spectra were measured *in-situ* to monitor degradation.

3. UV-visible absorption and Raman spectroscopy

UV-visible absorption spectra were acquired using a Shimadzu UV-2550 spectrophotometer. Raman spectra were recorded with five excitation wavelengths; 457, 488, 514, 633 and 785 nm with a Renishaw inVia microscope in back scattering configuration. Thin film samples were measured in a nitrogen-purged enclosed sample chamber. Precautions were taken to avoid photodegradation of the samples. The excitation conditions were: 785 nm (130 mW) with acquisition time 25 s, 633 nm (13 mW) 25 s, 514 nm (11 mW) 10–20 s, 488 (9.0 mW) 10–20 s, and 457 nm (1.6 mW) 1–10 s. The spectrometer was calibrated for frequency using a silicon reference sample. The background photoluminescence was subtracted using a polynomial fit after sampling at least three different regions in the sample.

4. Raman simulation

Raman spectra of thiophene oligomers were calculated using DFT at the B3LYP/6-31G* level of theory within the Gaussian 09 package.[34–39] In each case, the ground-state geometries of the molecules were first optimized in the gas phase (the hexyl side chains were replaced by methyl side groups to reduce computation time) and the Raman spectra of these optimized structures were then calculated (Figure SI.1[40]).

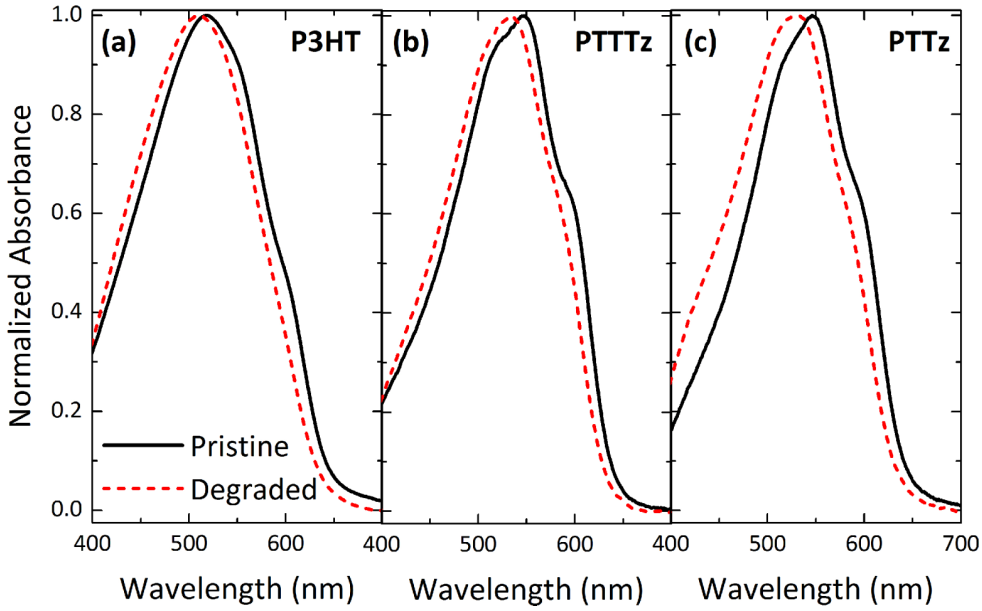

FIG. 2. UV-Visible absorption spectra for pristine (black solid line) and electrochemically degraded (red dashed line) films of P3HT, PTTTz, and PTTz.

III. RESULTS AND DISCUSSION

A. UV-visible absorption spectroscopy

The UV-Visible absorption spectra of pristine and electrochemically degraded (after polaron injection of ~10^{20} cm^3) films of the three polymers are shown in Figure 2. For the pristine polymer films, the absorption onsets are similar, indicating that the increasingly deeper HOMO energy level is accompanied by a deepening of the LUMO energy level such that the optical bandgap is unchanged. After the electrochemical degradation, there is a significant blue shift of the absorption onset and the peak position for all three polymers, and the absorption shoulder at around 590 nm is lost. These changes indicate an increase in conformational disorder in each case.[22] P3HT is the least blue-shifted (~7 nm) followed by PTTTz (~14 nm) and finally PTTz (~19 nm). The significant blue-shift for the polymer with the deepest HOMO energy level (PTTz) indicates that it experiences the strongest polaronic degradation effect.

B. Raman spectroscopy

A more detailed comparison of the molecular conformations for the three polymers is provided by the resonant Raman spectra (Figure 3). A resonant excitation (488 nm) was used to obtain a strong Raman scattering signal and enhanced sensitivity to morphological changes.[22] The resonant Raman spectra of conjugated molecules are typically dominated by a small number of vibrational modes describing stretches of the main conjugated backbone of the molecules. The vibrational modes of large molecules such as the polymers studied here typically involve nuclear motion of many atoms, thus producing collective motions of many bonds, but they can be understood more simply in terms of the dominant bond vibrations.

The Raman spectrum of P3HT is well known, and in this frequency range (1300-1600 cm^{-1}) consists of in-plane symmetric C—C (1380 cm^{-1}), symmetric C=C (at 1450 cm^{-1}), and anti-symmetric C=C (1525 cm^{-1}) stretching modes of the thiophene rings.[22,25,28–30,32] The full Raman spectra are provided in the supplementary material (Figure SI.0[40]). The new peaks that are only present in PTTTz and PTTz are assigned to the C—N (1331 cm^{-1}) and C=N (1501 cm^{-1}) stretch modes of the thiazole units in these polymers.[33] Increasing the number of thiazole units in the polymer backbone (from P3HT to PTTTz to PTTz) results in distinct differences in the Raman spectra (Figure SI.1[40]). We summarise below the effects of incorporation of thiazole units into a P3HT chain in its Raman spectrum.

(a) *Raman scattering intensities of the* C—N (1331 cm^{-1}) *and* C=N (1501 cm^{-1}) *modes increase relative to the* C—C *mode in PTTTz and PTTz*. Such an increase corresponds with the increased proportion of thiazole units in the polymer chain which these modes belong to.

(b) *Raman scattering intensity of the* C—C *mode* (1380 cm^{-1}) *reduces relative to the* C=C *mode* (1450 cm^{-1}) *in*

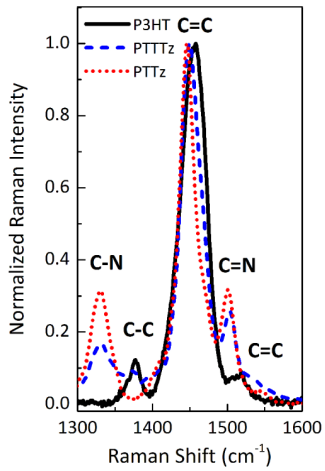

FIG. 3. Resonant Raman spectra for pristine thin films of P3HT, PTTTz, and PTTz measured under 488 nm excitation. Normalised to the strongest Raman peak (~1460 cm^{-1}).

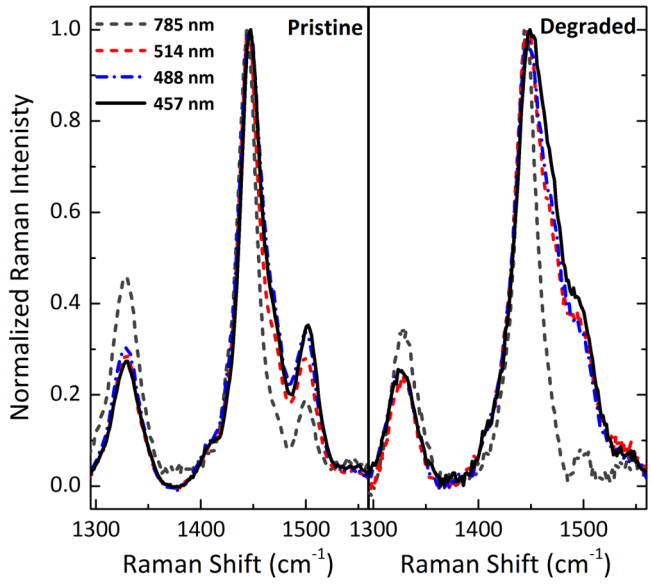

FIG. 4. Raman spectra of pristine and degraded films of PTTz measured with 457, 488, 514, and 785 nm excitations.

PTTTz and PTTz. The C—C bond is only found on thiophene units, but the C=C bond is present in both thiophene and thiazole, so the reduction in this ratio corresponds with the increasing proportion of thiazole units in the polymer chain. The apparent absence of this peak in PTTz, despite half of the units being thiophene, can be understood to indicate that the stretching modes of the thiazole ring have much larger Raman scattering cross sections under 488 resonant excitation than those in the thiophene unit (see a significant increase in the C—N and C=N mode intensities), or alternatively the C—C mode in the thiophene could shift to higher energy when adjacent to a thiazole unit, which would explain a slight increase in intensity of the shoulder observed at 1408 cm^{-1} in the PTTz spectrum.

(c) *The peak position of the main symmetric* C=C *stretch mode shifts to lower energy with increasing thiazole content* (*P3HT*—1456 cm^{-1}; *PTTTz*—1450 cm^{-1}; *PTTz*—1446 cm^{-1}). Shifts in the position of this mode towards lower energy (lower vibrational frequency) have previously been attributed to increases in planarity of the main conjugated backbone.[22,23,25,29,30,34] Here, we find that this effect correlates with an increase in the proportion of thiazole units, supporting the hypothesis that the reduced steric interactions between neighboring thiazole and thiophene units leads to increased planarity and longer effective conjugation length.[4] DFT geometry optimisation also supports this conclusion (see supplementary material for details[40]), predicting much smaller inter-unit torsion angle for PTTz (1°) than for P3HT (17°).

(d) *Width (FWHM) of the* C=C *symmetric stretch mode* (1460 cm^{-1}) *reduces with increasing thiazole content* (*P3HT*—39 ± 1 cm^{-1}, *PTTTz*—32 ± 1 cm^{-1}, *PTTz*—26 ± 1 cm^{-1}). A reduced FWHM indicates that the distribution of C=C modes in different conformational environments is narrower indicating an increase in energetic order.[22,35,36] The narrowing observed here when thiazole units are present is consistent with the increased backbone planarity mentioned above. This reduction in FWHM primarily results from a reduction in intensity in the higher energy part of this Raman peak, which is particularly associated with the disordered polymer phase, so this result indicates an overall increase in the degree of molecular order with increasing thiazole content.[22]

Raman spectroscopy is sensitive to the polarisability of molecules, which in turn depends upon the molecular conformation and effective conjugation length.[27,31,37] Therefore, the differences in the Raman spectra measured with different excitation wavelengths can provide information about particular morphological phases (ordered or disordered) present in the polymer samples studied here.[22] Figure 4 compares the Raman spectra of pristine and degraded PTTz films using several excitation wavelengths (785, 514, 488, and 457 nm).

The shorter wavelength excitations selectively probe more disordered portion of the polymer chains, corresponding with a relative shift in the main C=C peak position to higher energy.[22,30,25,23,38,28,32] As a result, the FWHM of the C=C peak for both pristine and degraded PTTz films increases with decreasing excitation wavelength (Figure 5). Figure 5 illustrates the maximum shift of the C=C mode and its FWHM value extracted from Figure 4. Importantly, for the degraded PTTz film a much larger increase in the FWHM of this C=C peak is observed relative to the pristine film (from 25.1 to

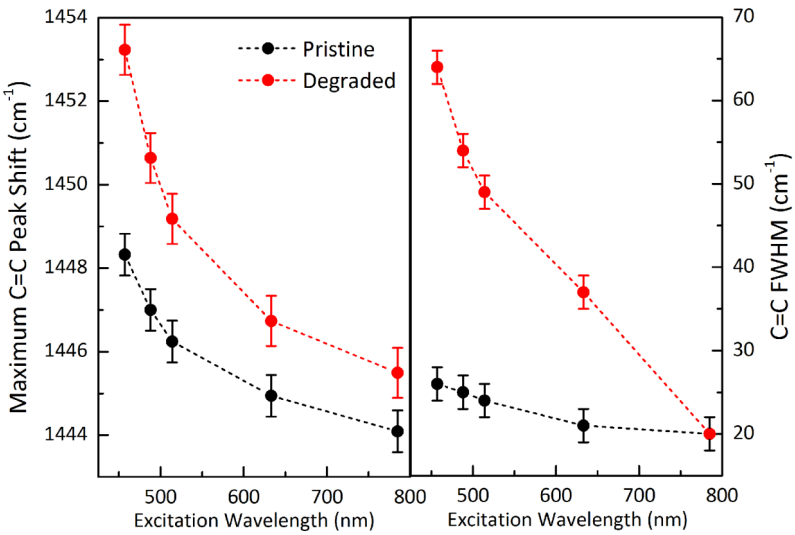

FIG. 5. Maximum peak position (cm^{-1}) and FWHM (cm^{-1}) of the main C=C mode in PTTz at 785, 633, 514, 488, and 457 nm excitations for pristine (black) and degraded (red) thin films.

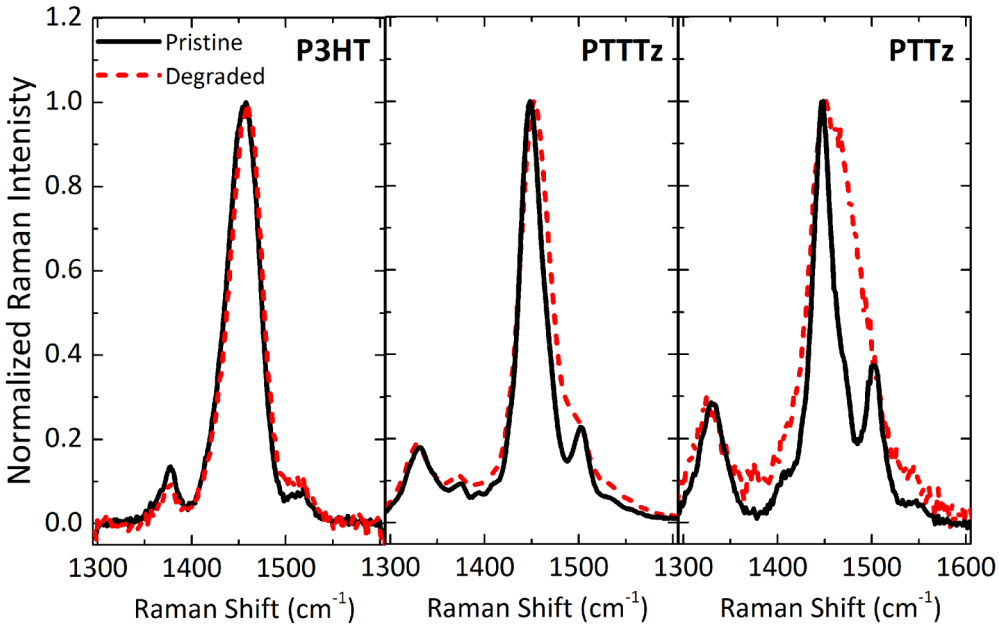

FIG. 6. Resonant Raman spectra for pristine (black solid line) and degraded films (red dashed line) of P3HT, PTTTz, and PTTz measured using 488 nm excitation.

64.0 cm^{-1} for 457 nm excitation). This is accompanied by an overall shift in the peak position to higher frequency (from 1446 to 1449 cm^{-1} for 457 nm excitation). Both the large increase in FWHM and the peak shift to higher frequency arise from an increased higher energy portion of the main C=C peak. This result clearly shows that the degradation mechanism induced by the electrochemical hole injection results in an increase in the fraction of disordered phase of the PTTz polymer, with reduced effective conjugation length potentially associated with increased inter-unit torsion angle (or breaking) of the conjugated polymer backbone.[22]

We now focus on the effect of electrochemical degradation on resonant Raman spectra of P3HT, PTTTz, and PTTz films.

The increase in the high energy component of the C=C stretching mode peak (~1460 cm^{-1}) is minimal for the P3HT film, though there is also a clear decrease in the intensity of the C—C stretch mode relative to the C=C peak, which indicates an increase in polymer disorder (Figure 6).[22] For the films where thiazole units have been incorporated into the chain (PTTTz, PTTz), the electrochemical degradation results in more significant changes, the most obvious being a larger increase in the high energy component of the main C=C vibration mode, showing that these polymers are more strongly affected. More subtle effects are detected using peak fitting to distinguish the contributions from the overlapping peaks.

We have fitted Lorentzians to the C—N (1331 cm^{-1}), $C{=}C_{Ordered}$ (1447 cm^{-1}), $C{=}C_{Disordered}$ (1464 cm^{-1}), and C=N (1501 cm^{-1}) peaks using fixed FWHM and peak centers (see Figure SI.2 in the supplementary material for details[40]). This allows us to extract ratios of the integrated peak intensities for the ordered and disordered components contributing to the C=C mode, providing a quantitative measure of the degree of polymer molecular order, and also to monitor degradation induced changes in the bonds involving the N atom. The I_{1447}/I_{1464} value is the ratio of the integrated intensities of the 1447 cm^{-1} peak (C=C in the ordered phase) to the 1464 cm^{-1} peak (C=C in the disordered phase). The I_{1501}/I_{1331} value is the ratio of integrated intensities of the C=N stretching mode (1501 cm^{-1}) to the C—N stretching mode (1331 cm^{-1}) (Table I).

In the pristine case, the I_{1447}/I_{1464} value is smallest for P3HT and increases with increased thiazole content (P3HT, 1.0; PTTTz, 4.2; PTTz, 7.0) confirming the increase in backbone coplanarity resulting from the thiazole unit. In all three polymers, the I_{1447}/I_{1464} value is largest for the pristine case and decreases once they are degraded, showing that the proportion of the disordered phase increases. In addition to these conformational changes induced by the electrochemical degradation, more specific information about particular bonds affected by this degradation can be gained from the relative intensities of the C—N (1331 cm^{-1}) and C=N (1501 cm^{-1}) vibrational modes. These bonds are only found in the thiazole unit so they are not observed for P3HT, but for both PTTTz and PTTz films this value (I_{1501}/I_{1331}) reduces after the sample

TABLE I. Relative peak intensity ratios (integrated) for the main vibrational modes of pristine and degraded P3HT, PTTTz, and PTTz films extracted from Lorentzian fits to Raman spectra measured with 488 nm excitation (Figure 6). Δ indicates the percentage change of the ratio after electrochemical degradation.

	P3HT			PTTTz			PTTz		
	Pristine	Degraded	Δ (%)	Pristine	Degraded	Δ (%)	Pristine	Degraded	Δ (%)
I_{1447}/I_{1464}	1.0 ± 0.2	0.7 ± 0.2	−30	4.2 ± 0.4	1.3 ± 0.2	−69	7.0 ± 0.5	1.1 ± 0.4	−85
I_{1501}/I_{1331}				0.43 ± 0.04	0.40 ± 0.04	−7	0.20 ± 0.02	0.13 ± 0.01	−28

is degraded. The significant decrease of C═N vs. C—N indicates that the electrochemical degradation affects the C═N bond more strongly than the C—N bond, and that the degradation mechanism involves either the p_z orbital of nitrogen or carbon. For PTTTz film, the integrated peak intensity of C═N vs. C—N remains mostly unchanged, whereas for the polymer containing the highest proportion of thiazole (PTTz) there is a significant reduction. In this instance, we would expect this degradation to cause a potential breaking of the C═N bond and hence reduce effective conjugation length and coplanarity of the polymer backbone in the degraded material. The electron donating nitrogen lone pair (in sp^2 orbital) could also have interactions with the cation part of the polaron, forming C—N bond and thus decreasing the C═N/C—N intensity value in the electrochemically degraded film. The reason why the nitrogen atom is particularly vulnerable to stability in the polaronic state is not yet clear, though we consider alternating thiophene-thiazole from the unsymmetrical hole polarons with high charge density in the C═N bond and nitrogen lone pair.[39] This leaves thiazole units more susceptible to radical degradation pathways centered on this site.

IV. CONCLUSIONS

Incorporation of thiazole units into a polythiophene polymer chain is understood to deepen the HOMO energy level and planarise the conjugated polymer backbone by reducing the steric hindrance between neighboring units. However, whilst the thiazole unit improves the chemical stability of the polymer in the ground state, the formation of the polaronic state shows increased susceptibility to electrochemical degradation, which is problematic for application in photovoltaic devices under normal operational conditions. In order to identify the mechanism of this degradation, we have employed resonant Raman spectroscopy. The Raman spectra of the three polymers (P3HT, PTTTz, and PTTTz) confirm a systematic enhancement of molecular planarity with increasing thiazole content. The presence of additional vibrational modes in the Raman spectra of PTTTz and PTTz related to the thiazole unit (C—N and C═N bond stretching modes) provides an important means to probe chemical changes associated to this unit during electrochemical degradation. We find that increasing the thiazole content in the thiophene chain makes the polymer more susceptible to degradation of hole polarons, resulting in a substantial increase in the conformationally disordered phase of the material. This is accompanied by a decrease in Raman scattering intensity of the C═N vibrational mode relative to the C—N mode, indicating the C═N bond is most vulnerable in the degraded polymer chain.

ACKNOWLEDGMENTS

The authors acknowledge funding provided by the EPSRC (Nos. EP/K029843/1, EP/I019278/1, EP/G031088/1, and DTA studentship) and Solvay SA.

[1]M. Jørgensen, K. Norrman, and F. C. Krebs, Sol. Energy Mater. Sol. Cells **92**, 686 (2008).
[2]M. Jørgensen, K. Norrman, S. A. Gevorgyan, T. Tromholt, B. Andreasen, and F. C. Krebs, Adv. Mater. **24**, 580 (2012).
[3]L. Huo, J. Hou, S. Zhang, H.-Y. Chen, and Y. Yang, Angew. Chem., Int. Ed. Engl. **49**, 1500 (2010).
[4]Y. Lin, H. Fan, Y. Li, and X. Zhan, Adv. Mater. **24**, 3087 (2012).
[5]D. M. de Leeuw, M. M. J. Simenon, A. R. Brown, and R. E. F. Einerhand, Synth. Met. **87**, 53 (1997).
[6]S. Sista, M.-H. Park, Z. Hong, Y. Wu, J. Hou, W. L. Kwan, G. Li, and Y. Yang, Adv. Mater. **22**, 380 (2010).
[7]J. Gilot, I. Barbu, M. M. Wienk, and R. A. J. Janssen, Appl. Phys. Lett. **91**, 113520 (2007).
[8]J. You, L. Dou, K. Yoshimura, T. Kato, K. Ohya, T. Moriarty, K. Emery, C.-C. Chen, J. Gao, G. Li, and Y. Yang, Nat. Commun. **4**, 1446 (2013).
[9]C.-H. Chou, W. L. Kwan, Z. Hong, L.-M. Chen, and Y. Yang, Adv. Mater. **23**, 1282 (2011).
[10]M. Manceau, A. Rivaton, and J.-L. Gardette, Macromol. Rapid Commun. **29**, 1823 (2008).
[11]M. S. A. Abdou and S. Holdcroft, Can. J. Chem. **1901**, 1893 (1995).
[12]N. Ljungqvist and T. Hjertberg, Macromolecules **28**, 5993 (1995).
[13]T. Caronna, M. Forte, M. Catellani, and S. V. Meille, Chem. Mater. **4756**, 991 (1997).
[14]M. Manceau, S. Chambon, A. Rivaton, J.-L. Gardette, S. Guillerez, and N. Lemaître, Sol. Energy Mater. Sol. Cells **94**, 1572 (2010).
[15]M. Koch, R. Nicolaescu, and P. V. Kamat, J. Phys. Chem. C **113**, 11507 (2009).
[16]A. Rivaton, S. Chambon, M. Manceau, J.-L. Gardette, N. Lemaître, and S. Guillerez, Polym. Degrad. Stab. **95**, 278 (2010).
[17]M. V. Madsen, T. Tromholt, A. Böttiger, J. W. Andreasen, K. Norrman, and F. C. Krebs, Polym. Degrad. Stab. **97**, 2412 (2012).
[18]H. Bronstein, M. Hurhangee, E. C. Fregoso, D. Beatrup, Y. W. Soon, Z. Huang, A. Hadipour, P. S. Tuladhar, S. Rossbauer, E.-H. Sohn, S. Shoaee, S. D. Dimitrov, J. M. Frost, R. S. Ashraf, T. Kirchartz, S. E. Watkins, K. Song, T. Anthopoulos, J. Nelson, B. P. Rand, J. R. Durrant, and I. McCulloch, Chem. Mater. **25**, 4239 (2013).
[19]D. Beatrup, J. Wade, L. Biniek, H. Bronstein, M. Hurhangee, J.-S. Kim, I. McCulloch, and J. R. Durrant, Chem. Commun. (Cambridge) **50**, 14425 (2014).
[20]T. Yamamoto, M. Arai, H. Kokubo, and S. Sasaki, Macromolecules **36**, 7986 (2003).
[21]E. Zaborova, P. Chávez, R. Bechara, P. Lévêque, T. Heiser, S. Méry, and N. Leclerc, Chem. Commun. (Cambridge) **49**, 9938 (2013).
[22]W. C. Tsoi, D. T. James, J. S. Kim, P. G. Nicholson, C. E. Murphy, D. D. C. Bradley, J. Nelson, and J. Kim, J. Am. Chem. Soc. **133**, 9834 (2011).
[23]S. Wood, J. S. Kim, D. T. James, W. C. Tsoi, C. E. Murphy, and J.-S. Kim, J. Chem. Phys. **139**, 064901 (2013).
[24]S. Wood, J. B. Franklin, P. N. Stavrinou, M. A. McLachlan, and J.-S. Kim, Appl. Phys. Lett. **103**, 153304 (2013).
[25]J. Razzell-Hollis, W. C. Tsoi, and J.-S. Kim, J. Mater. Chem. C **1**, 6235 (2013).
[26]W. C. Tsoi, D. T. James, E. B. Domingo, J. S. Kim, M. Al-hashimi, C. E. Murphy, N. Stingelin, M. Heeney, and J. Kim, ACS Nano **6**, 9646 (2012).
[27]C. Castiglioni, M. Tommasini, and G. Zerbi, Philos. Trans. R. Soc., A **362**, 2425 (2004).
[28]Y. Furukawa, AIP Conf. Proc. **1554**, 5 (2013).
[29]L. Brambilla, M. Tommasini, I. Botiz, K. Rahimi, J. O. Agumba, N. Stingelin, and G. Zerbi, Macromolecules **47**, 6730 (2014).
[30]A. Milani, L. Brambilla, M. Del Zoppo, and G. Zerbi, J. Phys. Chem. B **111**, 1271 (2007).
[31]C. Castiglioni, M. Del Zoppo, and G. Zerbi, J. Raman Spectrosc. **24**, 485 (2005).
[32]A. Milani, M. Tommasini, and G. Zerbi, J. Raman Spectrosc. **40**, 1931 (2009).
[33]S. E. Wiberley, N. B. Colthup, and L. H. Daly, *Introduction to Infrared and Raman Spectroscopy*, 3rd ed. (Academic Press, 1964).
[34]W. C. Tsoi, W. Zhang, J. R. Hollis, M. Suh, M. Heeney, I. McCulloch, and J.-S. Kim, Appl. Phys. Lett. **102**, 173302 (2013).
[35]X. Wang, D. Zhang, K. Braun, H.-J. Egelhaaf, C. J. Brabec, and A. J. Meixner, Adv. Funct. Mater. **20**, 492 (2010).
[36]S. Miller, G. Fanchini, Y.-Y. Lin, C. Li, C.-W. Chen, W.-F. Su, and M. Chhowalla, J. Mater. Chem. **18**, 306 (2008).
[37]B. Tian and G. Zerbi, J. Chem. Phys. **92**, 3892 (1990).
[38]S. Cook, A. Furube, and R. Katoh, Energy Environ. Sci. **1**, 294 (2008).
[39]J. Jordanov, J. Chem. Soc., Chem. Commun 743 (1975).
[40]See supplementary material at http://dx.doi.org/10.1063/1.4923197 for additional Raman spectra including peak fitting and further details of DFT calculations described in text.